

## HELIUM IN MATERIALS USE IN HYDROGEN CRYOGENIC DISTILLATION

**Sebastian BRAD, Mihai VIJULIE, Alin LAZĂR, Sorin GHERGHINESCU**

*National Institute of R&D for Cryogenics and Isotopes Technologies (ICIT)  
1000 - Rm. Valcea, Uzinei 4, CP10, Valcea, ROMANIA,  
phone:0040 250 736979, fax:0040 250 732746, e-mail: sebi@.icsi.ro*

**Abstract – Industrial plants that use cryogenic process like plants for liquid hydrogen distillation impose to use material with high tenacity that assures safety in working. The distillation part of a plant for tritium separation conducts to tritium implant in structure of the materials, mostly stainless steels.**

**Keywords:** cryogenic process, distillation, keyword c, keyword d, keyword e.

### 1. INTRODUCTION

An understanding of the behaviour of He in metals is important because He is generated in charged tritium storage media and in the structural materials of fission reactors, accelerators, breeders and future fusion reactors. Helium accumulation causes deterioration of the material properties and may influence the useful lifetime of reactor components. Helium effects in austenitic stainless steels have been studied extensively over the past decade. Therefore it is well known that austenitic stainless steels, which will be utilized for nuclear components, with small amounts of helium, suffered severe embrittlement accompanied by a change in structure mode from transgranular to intergranular.

### 2. GENERAL CONSIDERATIONS

For a full understanding of the changes of macroscopic mechanical properties due to helium, the microscopic quantities such as formation energy of interstitial (substitution) He,  $E_I^f$ , ( $E_S^f$ ), migration energy of interstitial He  $E_I^m$ , binding energy of two interstitial He atoms at one interstice,  $E_{2I}^b$ , binding energies of He vacancy,  $E_V^b$ , He-grain-boundary  $E_{GB}^b$ , and He-dislocation complexes  $E_D^b$ , activation energies for diffusion  $E_a$ , etc. should all be known. The relations between these quantities are:

- the formation energy for substitution helium,  $E_S^f$ , is the sum of the formation energy of an interstitially dissolved helium atom,  $E_I^f$ , and of the vacancy formation energy,  $E_V^f$ , minus the He-vacancy binding energy,  $E_V^b$ .

- the dissociation energy  $E_V^d$  of a He atom from a vacancy is the sum of the He-vacancy binding energy  $E_V^b$  and of the interstitial migration energy  $E_I^m$ .

In addition the following equation holds:  $E_V^d = E_I^f + E_I^m - E_S^f + E_V^f$ . Helium gas atoms have only transitional energy and in a regime of the ideal gas law, the following equations describe the chemical potential of one Helium atom in the gas phase.

$$\mu_{He}^{gas} = kT \ln\left(\frac{p}{kT} \frac{h^3}{(2\pi mkT)^{3/2}}\right) \quad (1)$$

and in the metal on substitution (S) sites

$$\mu_{HeV}^{metal} = H_S^f - TS_S^f + kT \ln\left(\frac{c_S}{1-c_S}\right) \quad (2)$$

or on interstitial (I) sites

$$\mu_{HeI}^{metal} = H_I^f - TS_I^f + kT \ln\left(\frac{c_I}{N-c_I}\right) \quad (3)$$

Here  $c_S$  and  $c_I$  are the ratios of He atoms on substitution and interstitial sites to the metal atoms,  $k$  is the Boltzmann constant,  $h$  is the Planck constant,  $m$  the mass of a He atom, and  $N$  gives the number of interstitial sites per metal atom. In the following, the term  $pV$  is neglected yielding  $E_I^f \sim H_I^f$  and  $E_S^f \sim H_S^f$ . Thermodynamic equilibrium yields the following equations:

$$c_S = \frac{h^3}{(2\pi mkT)^{3/2}} \frac{p}{kT} \exp\left(-\frac{E_S^f - TS_S^f}{kT}\right) \quad (4)$$

and

$$\frac{c_I}{N-c_I} = \frac{h^3}{(2\pi mkT)^{3/2}} \frac{p}{kT} \exp\left(-\frac{E_I^f - TS_I^f}{kT}\right) \quad (5)$$

For substitution occupation, the higher concentration value is caused by the lower substitution formation energy due, in turn, to the high binding energies  $E_V^b$  of He atoms to vacancies (for  $E_V^b > E_V^f$ ). As a consequence,  $c_S$  will always be much larger than  $c_I$ .

$$\frac{c_S}{c_I} = N \exp\left(-\frac{E_S^f \cdot E_I^f}{kT}\right) = N \exp\left(+\frac{E_V^b \cdot E_V^b}{kT}\right) \gg 1$$

At very high pressures, He deviates from ideal gas behaviour (assumed above) and the concentrations  $c_S$  and  $c_I$  may increase by even 3 to 4 orders of magnitude. This extremely low solubility of He are the reason for cluster or bubble formation even at small concentrations. Helium bubble formation requires diffusion of the He atoms. There are three different models for the migration of He in metals:

1. migration via jumps between interstitials sites. These processes should be similar to the diffusion of tritium in metals. Due to the large binding energy between Helium atoms and other defects, this type of diffusion can only occur in defect-free regions.
2. migration via the vacancy mechanism. The substitution Helium atom changes place with a vacancy in its immediate neighbourhood.
3. migration of He via the dissociation from a He-V complex and subsequent interstitial diffusion. The activation energy for this He diffusion process is  $E_a = E_V^d - E_V^f$ .

### 3. EXPERIMENTAL SETUP

Test stand modification by the elimination of the cryostat used for cooling, design for the sample specific polystyrene foam like a thermal protection envelope and the cryogenic liquid, make tension test at a specialized laboratory.

Concerning the objective of this research, we have to emphasize that the general experimental works has been developed onto the before designed equipment used for metallic toughness measurements in a large range of temperatures between 4 K until 300 K. The equipment has the facility to measure and control temperature with a high accuracy and also an automatic computer controlled data acquisition system.

In order to increase the accuracy of the testing and also to simplify the system, new polystyrene foam has been used as a thermal protection envelope instead of the complicated and hard to be used cryostat. A general view of this improvement of our resilience testing device could be seen below where the polystyrene jacket, replace the entire cryostat.

It is well-known that the main parameter for materials used for designing and building the cryogenic installation is the resilience, which is the absorbed energy at breaking. Therefore, the toughness measurements have been made at three temperature levels, shown in the results tables.

Three types of materials have been investigated using Charpy machine, both with the old toughness measurement system and the improved one. The measuring conditions have been kept the same during both experimental systems. Also, the data acquisition automatic line has been used for both measurements sets.

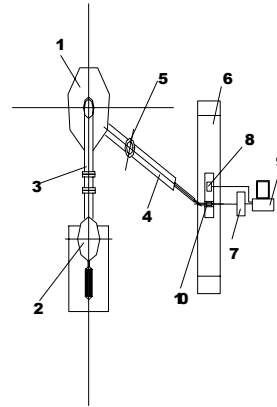


Figure 1: Experimental system

The main elements which compose the experimental stand are:

1. Cold-box – inside is the cryostat for the cryogenic liquid (in our case liquid hydrogen)
2. Liquid hydrogen cryogenerator type PPH
3. Cryogenic liquid transfer line (between PPH and Cold-Box)
4. Cryogenic liquid transfer line (between Cold-Box and Charpy device)
5. Cryogenic valve
6. Resilience testing machine
7. Temperature A/D acquisition system
8. Resilience A/D acquisition system
9. Process computer
10. Polystyrene jacket



Figure 2: The experimental stand

Inside of the Cold-Box we design a cryogenic liquid holder in order to accumulate a hold-up enough for several resilience tests. The liquid hydrogen cryogenerator is a Phillips machine type A20 which

can make two energy temperature levels at 80K and 20 K. The cold escape rate was calculated and there are, for liquid hydrogen, between 3W to 5W depending the temperature of the PPH cooling water. For the calculated value of the warming amount exchange between two surfaces, A1 cold surface and A2 the warm surface which surround the first one, we taken into account the value of the free way of particole 1 and the distance between cold and warm surfaces, d.

The important element of this new version of resilience testing stand is the polystyrene Jacket. The liquid hydrogen transportation in the jacket is made by a thin copper tube. Inside of the jacket there is enough space in order to enter the cryogenic liquid in order to have a slow and uniform cooling of the sample.

The breaking machine used for the new version of this stand was Charpy F040/S equipped with resilience A/D acquisition system.

Differences between the older versions consist in the method of the temperature achievements for the sample in order to not modify, even for few seconds, the parameters of the breaking tests. For the old version of the testing stand, the samples, after were cooled down at a lower temperature than the breaking one, they were moved from the cryostat, to the Charpy testing machine zone. In that time there is an uncontrolled warming up of the sample, corrected with a factor of temperature without a very good control of the conditions of the ambient temperature.

With the jacket used for each breaking sample, we can control with a good accuracy the value of the temperature. The measurement of the temperature was made it in two different ways. The first method use a temperature stamp putted on the surface of the sample but in this case we break the sample at different temperatures between the surface and the bulk.

Therefore we chose the method of a thermocouple type E, put inside of a hole drilled in the sample, which measure the temperature of the bulk of the sample. The values of resilience obtained, in this case, will be modified with a factor determinate by the tension factor induce by the drilled hole. Also on these values we must taken into account the value of the toughness of the jacket (at low temperature level we consider zero this value).

The new version of breaking testing stand could be also used at liquid helium. In this configuration, at the Cold-Box, a specialized liquid helium Dewar can be connected. For the tests we use in this case the same configuration with a little differences for the temperature measurement sensor.

#### 4. EXPERIMENTS

For influence oh helium on different materials was chosen two different types of stainless steel:

Type	C %	Si %	Mn %	P %	S %	Cr %	Mo %	Ni %
W1.4006 (X10Cr13)	0,08-0,12	1	1	0,045	0,030	12-14	-	-
W1.4404 (X2CrNiMo18 10)	≤0,03	1	2	0,045	0,030	16,5-18,5	2-2,5	11,0-14,0

Table 1: The types of stainless steel

For each stainless steel we have a programme of investigation in order to determine the influence of corrosion factors, helium and internal defects, on the proprieties of materials at different temperatures. The samples was cooled down at -200°C and broken in order to observe the influence on the toughness. With XRD analysis was determinate the concentration of the Fe $\alpha$ % and Fe $\gamma$ %. The other components were induced by a corrosion treatment in diluted solution of HCl (18.3%) or HNO<sub>3</sub>(27.7%). The entire components obtain in the materials decrease strongly the toughness of the steels, with values comprises in 10-30%. For two samples of W1.4006 was induced a surface mechanical treatment (work hardening) in order to modify the dislocation concentration. The work hardening of a crystalline material is a complex phenomenon, because the stress necessary to move a dislocation depends both on short-range interactions such as the intersection of forest dislocations, and long-range interactions with both near and distant dislocations. Despite a considerable research effort in this area, a complete understanding of the subject has not yet been achieved, even for single crystals. The problem is in two parts. First, the variation of dislocation content with strain must be determined. Second, the dependence of the flow stress on the dislocation content must be determined. For this sample was observed an increase of the toughness and mechanical resistance, in correlation with the increase value of the dislocation concentration (dislocations induced by the rolling mechanical process applied to the samples)

Material	Temp. (K)	Energy (J)
W1.4006(not treated sample)	300	112
W1.4006(not treated sample)	73	92
W1.4006 (treated sample in acid)	73	80
W1.4006 (treated sample in helium)	73	90
W1.4006 (work hardening)	73	95
W1.4404(not treated sample)	300	145
W1.4404(not treated sample)	73	102
W1.4404(treated sample in acid)	73	99
W1.4404(treated sample in helium)	73	98

Table 1

## 5. MEASUREMENTS

Data acquisitions were made with a DRON UM1 diffractometer connected with PC. A horizontal powder goniometer in Bragg-Brentano geometry with graphite monochromator was used. The incident Cu- $K_{\alpha}$  radiation,  $\lambda = 1.54178 \text{ \AA}$  was used. The typical experimental conditions were: 2 sec. for each step, range angle  $2\theta = 10^{\circ}$ - $100^{\circ}$ , step  $0.05^{\circ}$ . The spectra obtained in these conditions were used to make qualitative and quantitative phase analysis and to determine the microstructure parameters by whole pattern fitting method [1-3].

Type	Code	Sample description
W1.4006	4006_eta	Etalon: Cr (12-14%), Si (1%), Mn (1%), S (0.03%), P (0.045%), C (0.08-0.12)%, restul Fe
W1.4006	<b>W1_4006</b>	W1.4006/HCl/30min./470grd/1h
W1.4006	W1_4006a	W1.4006/.../790-820°C /30min/HCl
W1.4006	W1_4006b	W1.4006/He/740-820°C /30min/HNO3
W1.4006	W_4006c	W1.4006/HNO3
W1.4006	W_4006b	W1.4006/He/750-820°C /30min.

Table 3

Type	Code	Sample description
W1.4404	4404_eta	Etalon: Cr (12.5-18.5%), Ni (11-14%), Mo (2-2.5%), Si (1%), Mn (2%), S (0.03%), P (0.045%), C under 0.03%, Fe
W1.4404	<b>W1_4404</b>	W1.4404/He/1050 °C/1h
W1.4404	W1_4404a	W1.4404/H2/30 min/500 °C /HNO3
W1.4404	W1_4404b	W1.4404/HCl/12 h/H2/30min/470 °C
W1.4404	W1_4404c	W1.4404/1050 grd/5-10 min/He/470 °C

Table 3

Qualitative phase analysis on W1.4006 and W1.4404 of the presence of  $Fe\alpha$  (martensite) and  $Fe\gamma$  (austenite) is presented in table 5. The estimated concentrations are provided by analysis of figures of diffraction pattern.

Samples W1.4006	Concentrations estimated of $Fe\alpha\%$ and $Fe\gamma\%$	Samples W1.4404	Concentrations estimated of $Fe\alpha\%$ and $Fe\gamma\%$
4006_eta	0% and 100%	4404_eta	100% and 0%
W1_4006	<1% and >99%	<b>W1_4404</b>	<10% and >90%
W1_4006a	~50% and ~50%	W1_4404a	<1% and >99%
W1_4006b	<10% and >90%	W1_4404b	~100% and ~0%
W_4006c	~100% and ~0%	W1_4404c	>99% and <1%
W_4006b	~100% and ~0%		

Table 5

Etalon W1 4404 35KV 30mA CuKa 10-100 0.05, 2s grafit 20-100 grd et2\_brad

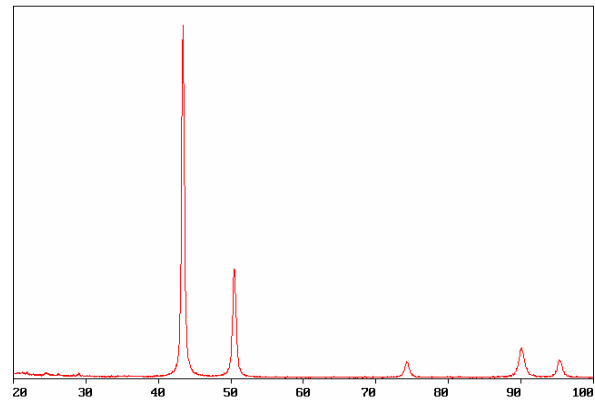


Figure 3: Etalon XRD spectra for W1.4404

Etalon W1 4006 35KV 30mA CuKa 40-100 0.05, 2s grafit 10-100 grd et1\_brad

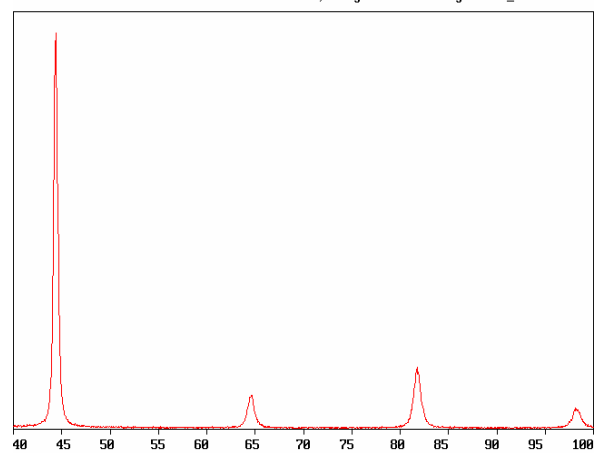


Figure 4: Etalon XRD spectra for W1.4006

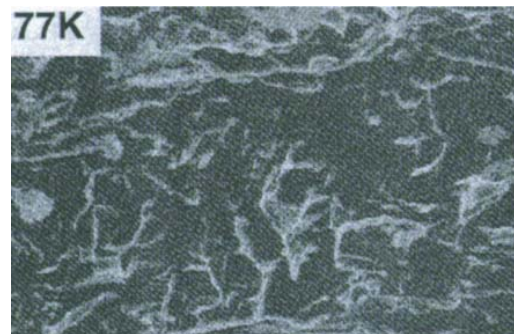


Figure 5: SEM on a breaking surface

It could be seen the many nuclear cavities from which ridges emanate. The morphology of internal voids and cracks, in helium embrittled steels, leaves little doubt that growth commonly occurs by the development of new surface progressively at the roots of notches because broad expanses of relatively smooth surface are exposed. Fracture studies using the scanning electron microscopy seem to place the sites of cavity nucleation too far apart in relation to the height of the ridges of final rupture, as could be

seen in the figure. Fracture has followed grain boundaries.

The mechanical proprieties of the materials decrease for the samples treated in corrosive and helium atmosphere (Table 2). Helium can influence the behaviour of materials significantly. The helium embrittlement suffered is also accompanied by a change in structure mode from transgranular to intergranular. A consequence of the extremely low solubility of He are the reason for cluster or bubble formation even at small concentrations. Helium bubble formation requires diffusion of the He atoms. The role of the helium in fracture mechanism is that of a perturbation on the basic strength of the metals. Theoretically strength we can consider the maximum strength obtained for the laboratory defect-free metal whiskers. For industrial metals and also for small strains these systems approximate elastic behaviour, but the bulk of the stress-strain curve is discussed in terms of glissile dislocations and their interactions.

For the samples with work hardening treatment, the subsequent deformation of the material, dislocation pile-ups will occur not only at grain boundaries, but at other obstacles formed during the deformation, e.g. sessile dislocations such as the Lomer-Cottrell barrier in FCC materials. Several work hardening theories based on the long-range stresses from dislocation pile-ups have been formulated. At a sufficiently large applied stresses, the barriers to slip will either be overcome, or broken by the dislocations, and the rate of work hardening will be reduced.

Further more small changes in the chemical composition, the grain size, the degree of plastic constraint caused by a notch or flaw, and even the rate at which a load is applied can all have a marked strength, toughness, and the temperature at which the ductile-to-brittle transformation occurs.

## 6. CONCLUSIONS

For the influence of helium and internal defects, the use body-centred-cubic metals at low temperatures

have to be under taken with considerable care increasing with any other external or internal factors. An important reason for why we propose a studies of the comportment and movements of helium and dislocations in a body-centred-cubic is that the ferritic and martensitic steels are cheaper than the austenitic steels and we can expect than for a group of parameters tables and data compilations that we obtained with this study, we found how we can lower the temperature at which a certain grade where those steels may be employed safely. The process of the influence of these factors an especially the dislocation influence on the material proprieties at low temperature will be investigate with Leed-Auger investigation technique.

## References

- [1] B. E. Warren, *X-Ray Diffraction*, (Reading MA Addison-Wesley), 1969.
- [2] B. E. Warren and B. L. Averbach, *J. Appl. Phys.* 21, 1950.
- [3] C. Ducu, V. Malinovschi, I. Iosub, *Revue de Chimie*, 54, 8, 2003.
- [4] K. S. Forcey, D. K. Ross, J. C. B. Simpson and D. S. Evans, *J. Nucl. Mater.* 160, 1988.
- [5] E. Serra, A. Perujo and G. Benamati, *J. Nucl. Mater.* 245, 1997.
- [6] E. Serra and A. Perujo, *J. Nucl. Mater.* 240, 1997.
- [7] K. Kizu, A. Pisarev and T. Tanabe, *J. Nucl. Mater.* 289, 2001, p. 291-302.
- [8] T. Shiraishi, M. Nishikawa, T. Yamaguchi and K. Kenmotsu, *J. Nucl. Mater.* 273, 1999, pp. 60-65.
- [9] A. A. Yukhimchuk and V. K. Gaevoy, *J. Nucl. Mater.* 233-237, 1996, pp. 1193-1197.
- [10] R. Lasser, *Tritium and Helium-3 in Metals*, Springer Series in Materials Science